

AD-A137 231

PARTICLE SCATTERING STUDIES ON FOREIGN IONS IN  
SUPERIONIC CONDUCTORS(U) STATE UNIV OF NEW YORK AT  
ALBANY DEPT OF PHYSICS W L ROTH ET AL. 21 DEC 83 TR-1  
N00014-82-C-0559

1/1

UNCLASSIFIED

F/G 7/4

NL

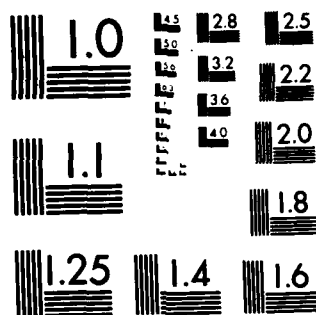
END

DATE

FILED

2-84

DTIC



MICROCOPY RESOLUTION TEST CHART  
NATIONAL BUREAU OF STANDARDS-1963-A

AD A 137231

13

OFFICE OF NAVAL RESEARCH

Contract N00014-82-0559

Task No. NR 627-833

TECHNICAL REPORT NO. 1

Particle Scattering Studies on  
Foreign Ions in Superionic Conductors

by

W. L. Roth, R. E. Benenson, C. Ji, L. Wielunski and B. Dunn

Prepared for Publication

in

Proceedings of the 4<sup>th</sup> International Conference on Solid State Ionics

and to be published

in the

Journal Solid State Ionics

State University of New York  
Department of Physics  
Albany, NY 12222

December, 1983

Reproduction in whole or in part is permitted for  
any purpose of the United States Government

Approved for Public Release; Distribution Unlimited

DTIC FILE COPY

DTIC  
SELECTE  
JAN 26 1984  
S D

84 01 26 006

REPORT DOCUMENTATION PAGE		READ INSTRUCTIONS BEFORE COMPLETING FORM
1. REPORT NUMBER	2. GOVT ACCESSION NO.	3. RECIPIENT'S CATALOG NUMBER
	AD-A137231	
4. TITLE (and Subtitle)		5. TYPE OF REPORT & PERIOD COVERED
Particle Scattering Studies on Foreign Ions in Superionic Conductors		Technical Report #1
		6. PERFORMING ORG. REPORT NUMBER
7. AUTHOR(s)		8. CONTRACT OR GRANT NUMBER(s)
W. L. Roth, R. E. Benenson, C. Ji., L. Wielunski and B. Dunn		C N00014-82-0559
9. PERFORMING ORGANIZATION NAME AND ADDRESS		10. PROGRAM ELEMENT, PROJECT, TASK AREA & WORK UNIT NUMBERS
Department of Physics State University of New York Albany, NY 12222		NR 627-833
11. CONTROLLING OFFICE NAME AND ADDRESS		12. REPORT DATE
Office of Naval Research, Chemistry Program, Code 472, 800 N. Quincy, Arlington, VA 22217		21 December 1983
		13. NUMBER OF PAGES
		16 plus 7 figures
14. MONITORING AGENCY NAME & ADDRESS (if different from Controlling Office)		15. SECURITY CLASS. (of this report)
		15a. DECLASSIFICATION/DOWNGRADING SCHEDULE
16. DISTRIBUTION STATEMENT (of this Report)		
This document has been approved for public release and sale; its distribution is unlimited.		
17. DISTRIBUTION STATEMENT (of the abstract entered in Block 20, if different from Report)		
18. SUPPLEMENTARY NOTES		
19. KEY WORDS (Continue on reverse side if necessary and identify by block number)		
Solid Electrolytes, Ion Implantation, Rutherford Backscattering, Nuclear Reaction Analysis, Channeling		
20. ABSTRACT (Continue on reverse side if necessary and identify by block number)		
<p>→ The effects of foreign ions on the structures and properties of superionic conductors are being investigated. This paper reports Rutherford backscattering, nuclear reaction analysis, and channeling studies on Na<math>\beta</math>-alumina crystals doped with Mn by ion implantation and with Li and Mg from melts. Implantation disorders the Na<math>\beta</math>-alumina surface. On heating, the surface crystallizes, and Mn diffuses into Al sites. The melt-doped compositions are accounted for by Mg substitution in the spinel layer and by Li in the conduction plane. →</p>		

Particle scattering has been used to profile sodium and impurities in Na<sub>2</sub>-alumina ceramics and F disorder in  $\text{Ba-PbF}_2$ . ←

*beta*

*beta*

Accession For	
NTIS GRA&I	<input checked="" type="checkbox"/>
DTIC TAB	<input type="checkbox"/>
Unannounced	<input type="checkbox"/>
Justification	
By _____	
Distribution/	
Availability Codes	
Dist	Avail and/or Special
<i>A/1</i>	



## PARTICLE SCATTERING STUDIES ON FOREIGN IONS IN SUPERIONIC CONDUCTORS

W.L.Roth, R.E. Benenson, C. Ji, and L. Wielunski

Physics Department, State University of New York, Albany, NY 12222

and B. Dunn, University of California, Los Angeles, CA 90024

### ABSTRACT

The effects of foreign ions on the structures and properties of superionic conductors are being investigated. This paper reports Rutherford backscattering, nuclear reaction analysis, and channeling studies on Na $\beta$ -alumina crystals doped with Mn by ion implantation and with Li and Mg from melts. Implantation disorders the Na $\beta$ -alumina surface. On heating, the surface crystallizes, and Mn diffuses into Al sites. The melt-doped compositions are accounted for by Mg substitution in the spinel layer and by Li in the conduction plane. Particle scattering has been used to profile sodium and impurities in Na $\beta$ -alumina ceramics and F disorder in  $\beta$ -PbF<sub>2</sub>.

## PARTICLE SCATTERING STUDIES ON FOREIGN IONS IN SUPERIONIC CONDUCTORS

W.L.Roth, R.E. Benenson, C. Ji, and L. Wielunski

Physics Department, State University of New York, Albany, NY 12222

and B. Dunn, University of California, Los Angeles, CA 90024

### Introduction

The structure, conductivity, and stability of superionic conductors can be changed by incorporating additives and impurities in solid solution. In many cases, the added element is an essential component of the atomic arrangement, and it must be present to obtain the phase with the desired properties. Examples of essential foreign ions are Ca and Y in calcia-stabilized zirconia and Li and Mg in Na $\beta$ -alumina. In the former, as a result of substituting divalent and trivalent cations for tetravalent zirconium, vacancies are introduced into the anion sublattice, and ionic currents can then be carried by oxygen hopping between occupied and vacant sites. In the latter, Na $\beta$ -alumina is metastable in binary compositions and 'stabilized' by the substitution of Li and Mg for Al in the spinel layer. Undesirable impurities may be introduced in the raw materials or from the environment. Examples of undesirable ions in Na $\beta$ -alumina are calcium, which inhibits ionic conductivity, and iron, which is a source of electrons for electronic conductivity.

A variety of experimental techniques can be used to dope superionic conductors. Foreign ions may be built into the lattice at the time of crystal growth by incorporating them in the raw materials.

After the crystals are grown, dopants may be introduced by diffusion at high temperature, ion exchange in molten salts, and implantation with high energy ions from an accelerator. The various methods insert the foreign ion in different crystallographic sites and result in materials with different properties.

An unique feature of ion implantation is its potential for introducing a wide variety of ions with different electronic structures into crystallographic sites that are not accessible by thermal methods. The implanted ions have a range of a fraction of a micron to a few microns and are studied by near-surface techniques, such as Rutherford backscattering (RBS) and nuclear reaction analysis (NRA). A consequence of implantation is lattice and structure disorder in the surface layers, which can be investigated using alpha particle and proton channeling.

This paper reports surface studies on  $\text{Na}\beta$ -alumina that was doped during crystal growth and by ion implantation. We also describe the use of these techniques to measure depth concentration profiles of impurities in the near-surface layers of  $\text{Na}\beta, \beta'$ -alumina ceramics and to study structure disorder in  $\beta\text{-PbF}_2$  crystals.

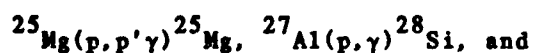
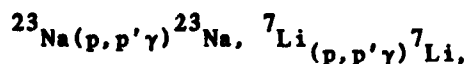
### Experimental

Ion implantation and particle scattering experiments were performed at the Accelerator Laboratory of SUNY-Albany. RBS spectra were collected using 2 and 3 MeV  $\alpha$  particles. Atomic composition ratios in the surface were obtained from the ratios of step-edge heights and the Rutherford scattering cross sections. Concentration



changes in  $\beta$ -alumina were followed to depths of a few thousand angstroms below the surface using 2 MeV alpha particles and to depths of several microns using 1.9 MeV protons. Methods for interpreting particle scattering measurements are given in Ref (1).

The compositions of monocrystals and ceramics of Na $\beta$ -alumina and Na $\beta'$ -alumina were determined by means of the nuclear reactions



detected. Pb and F in PbF<sub>2</sub> was determined by simultaneous measurement of elastic backscattering and the



Axial channeling widths and backscattering yields were measured using a two-axis goniometer. The Na $\beta$ -alumina crystals tended to charge in the ion beam. To prevent surface damage, the positive charge was neutralized with a beam of electrons directed from a heated filament near the crystal. The goniometer was equipped with a furnace that could be heated to make in situ measurements to temperatures above 400°C without exposing the specimen to the atmosphere.

Manganese was implanted in Na $\beta$ -alumina slabs cut from a Carbon and Carbide Co. crystal boule. The implantations were made in a direction approximately parallel to <0001> with 110 keV ions of <sup>55</sup>Mn. The implanted dose ranged from 0.1 to 1.1x10<sup>17</sup> Mn<sup>+</sup>/cm<sup>2</sup>.

The crystals for implantation were cut with a string saw into 4x8mm slabs, about 0.5 mm thick. Portions of the crystal were shielded from the ion beam so that RBS and channeling measurements could be made on

implanted and unimplanted areas.

Lithium and magnesium doped  $\text{Na}\beta$ - and  $\text{Na}\beta'$ -alumina crystals were grown by isothermal evaporation of  $\text{Na}_2\text{O}$  from melts at  $1695^\circ\text{C}$ . The melts were doped with Li, Mg, and Li+Mg mixtures. Crystal growth details and conductivity measurements have been reported (2).

#### Melt-Doped Beta Aluminas

The various methods of introducing foreign ions into  $\text{Na}\beta$ -alumina produce widely differing results, in large part because of its unique layer structure. The Al-O framework comprising the spinel layer is held together by strong ionic bonds, and reactions requiring mass transport, such as diffusion and sintering, are slow at temperatures below  $1500^\circ\text{C}$ . In contrast, the bonds to sodium in the conduction plane are very weak, and ion exchange reactions are rapid at temperatures as low as  $300^\circ\text{C}$ . The doping experiments described in this section were carried out at  $1695^\circ\text{C}$ , at which temperature diffusion is rapid; the site locations are determined by the thermodynamic activities of the ions in the crystal and in the melt.

Since the classic work of Kummer et al. (3), it has been known that  $\text{Li}^+$  and  $\text{Mg}^+$  can be incorporated in the  $\beta$  and  $\beta'$  alumina crystal structures. This section briefly reviews the compositions of mixed (Li-Mg)- $\beta$  and  $\beta'$  aluminas as an example of the use of NRA to determine the concentration of dopants in a single small crystal.

Table I gives the composition determined by NRA near the surface of Na- $\beta$  and Na $\beta'$ -alumina crystals, grown from melts doped with different Li/Mg ratios. The stoichiometries are expressed as atoms per spinel block and compared with that of a Carbon and Carbide Na $\beta$ -alumina crystal.

TABLE I

COMPOSITION OF MELT-DOPED BETA ALUMINAS

<u>Atom Ratio</u>	<u>Phase</u>	<u>Beta</u>	<u>Beta'</u>	<u>Beta''</u>
Mg/Li	Melt	0.5	1.0	
	Solid	3.0	40.0	
Mg/Al	Melt	0.015	0.031	0.13
	Solid	0.051	0.077	0.083
Li/Al	Melt	0.030	0.030	0
	Solid	0.017	0.002	0

Table I shows that both Na $\beta$ - and  $\beta'$ -alumina can accommodate a substantial number of Mg atoms in their structure. The Mg content increases with the Mg concentration in the melt. The number of Mg appears to be approaching an asymptotic limit of one Mg per spinel

block, regardless of whether the crystal has the  $\beta$  or  $\beta^*$  alumina crystal structure. By contrast,  $\text{Na}\beta$ -alumina accepts only moderate quantities of Li, and  $\text{Na}\beta^*$ -alumina accepts practically none at all.

The partition of Li and Mg between the two different crystal structures is determined by the ratio of their activities in the solid and the melt. Assuming that doping depends primarily on the stability of the ion in the solid, which is by no means certain, the partition of the additives suggests that Mg is more stable in the spinel layer and Li is more stable in the conduction plane. It is known from neutron diffraction that Mg (4) and Li (5) replace Al to reduce local stress in the center of the spinel layer, and the same substitution is expected to occur in  $\text{Na}\beta$ -alumina. The failure to grow crystals of Li-stabilized  $\beta^*$  alumina can be explained by instability of the ternary compound in equilibrium with the melt.

#### Mn-implanted $\text{Na}\beta$ -alumina

The results of using ion implantation to introduce foreign ions in a superionic conductor will now be given.  $\text{Na}\beta$ -alumina was chosen for an exploratory study of the potential for doping superionic conductors by ion implantation because a great deal is already known about substitutional and interstitial defects in its structure (4). Mn was selected as the foreign ion to be implanted because it is a transition element with well known electronic and optical properties, and its high atomic number is an advantage for profiling and an intended subsequent structure analysis with SEXAFS.

Fig 1 displays RBS spectra of a  $\text{Na}\beta$ -alumina crystal directly

after Mn implantation, after annealing at  $1100^{\circ}\text{C}$  for 1/2 hr, and then after annealing at  $1100^{\circ}\text{C}$  for 25 hrs. The Mn dose was  $1.1 \times 10^{17} \text{ Mn}^+/\text{cm}^2$ , implanted at 110 keV normal to the cleavage face.

The projected range of the Mn, estimated from the energy shift of the Mn edge upon tilting the target away from normal incidence, was about 700A. The implanted atoms introduced substantial disorder into the Na $\beta$ -alumina surface, which can be seen from enhanced backscattering of Al in RBS spectra measured with the ion beam in a direction aligned with the  $\langle 0001 \rangle$  axis of the crystal. Fig 2 Fig 3 compare the spectra measured on a Na $\beta$ -alumina crystal, before and after implantation. The broad Al peak on the aligned spectrum of the implanted crystal is caused by a disordered layer that is not in atomic register with the underlying substrate. The depth of the disordered layer, estimated from the width of the peak, is about 1500A, twice the projected range of the Mn ions.

When an incident particle beam lies nearly along the axis of a good crystal, the particles are steered away from close encounters and the number of nuclear collisions is reduced. The result is that the scattering by Coulomb collisions at angles almost  $180^{\circ}$  with respect to the incident beam is much reduced, yielding a minimum RBS yield in a narrow angular interval. This channeling was used to investigate the structural damage in the surface by determining the angular dependence of the alpha particles backscattered from Al and Mn atoms when the incident beam was nearly aligned with the  $\langle 0001 \rangle$  axis. The minimum yield, termed  $\chi_{\text{min}}$ , ranges from a very few percent

of the yield for a random incident ion direction for a perfect crystal to values approaching 100% for a nearly amorphous layer. An indication of the amount of damage introduced into a crystal is provided by the yield at the minimum in the backscattering spectrum of the unimplanted and implanted crystal, as shown in Fig 4. The backscattering yield for Al atoms in the unimplanted crystal is given by the angular channel width  $\Psi = 1.0^\circ$  and the backscattering minimum yield  $\chi_{\min} = 5\%$ . The corresponding channeling yields measured on the implanted crystal are  $\Psi = 1.0^\circ$  and  $\chi_{\min} = 45\%$ . The dechanneling is evidence for a substantial number of interstitial atoms in the surface. The angular dependence of the Mn yield across the channel gave no indication of channeling, from which we conclude that Mn is more or less randomly distributed in the surface.

Theoretical channeling widths and minimum yields have been estimated for a simplified model of the Na $\beta$ -alumina lattice. Taking an average spacing for the Al-O rows parallel to the c-axis, an average isotropic Debye parameter for Al and O from diffraction data, and neglecting the contributions of sodium and oxygen in the conduction plane, the predicted channeling width and backscattering minimum yield are  $\Psi = 0.8^\circ$  and  $\chi_{\min} = 5.7\%$ . The experimental yield and channeling width in unimplanted Na $\beta$ -alumina is in reasonable agreement with the theory, considering the approximations that were introduced in order to make the theoretical calculation.

We now discuss the processes that take place in the implanted

surface during annealing. The channeling spectrum in Fig 5 shows that annealing causes the Mn to spread out and diffuse toward the surface, as shown by the broadening of the peak and the shift of the Mn edge to higher energy. At the same time, the disappearance of the disorder peak in the aligned RBS spectrum, and an increase of  $\chi_{\min}(\text{Al})$  to 55%, means that the damaged layer has recrystallized into small, slightly misoriented, crystalline regions. Turning now to Fig 4, we estimate from  $\chi_{\min}(\text{Mn})=85\%$  that about 33% of the Mn atoms have substituted in Al sites. After a 25 hr anneal, the Mn substitution increased to about 100%. After heating at  $1500^{\circ}\text{C}$ , Mn could no longer be detected in the surface and there was a substantial improvement in the perfection of the surface structure, as shown by  $\chi_{\min}(\text{Al})=25\%$ . At this time it is not known whether the Mn vaporized or, as a result of diffusion, was present in the surface at a concentration too small to detect.

Table II summarizes the channeling yields determined for implanted and annealed crystals. The first column gives the heat treatment and the second and third columns the backscattering minimum yields for Al and Mn. The fourth column is an estimate of the fraction of Mn atoms that have substituted for Al.

TABLE II  
CHANNELING YIELDS

Na $\beta$ -alumina implanted with Mn and annealed. The Mn dose was  $1.1 \times 10^{17}$  Mn<sup>+</sup>/cm<sup>2</sup>, as measured by RBS.

<u>Heat Treatment</u>	<u><math>\chi_{\min}^{\text{Al}}</math></u>	<u><math>\chi_{\min}^{\text{Mn}}</math></u>	<u>Remarks</u>
Cleaved crystal	5		Unimplanted
Implanted crystal	45	100	Mn random
1100C 1/2 hr	55	85	33% substitution
1100C 25 hr	59	59	100% substitution
1500C 1 hr	25	?	Mn not detected

Applications to Ceramics

Particle scattering has been used to investigate several different phenomena in superionic conductors, and we mention here studies on Na $\beta$ -alumina ceramics (6) and  $\beta$ -PbF<sub>2</sub>.

For technological applications, solid electrolytes are used in the form of thin-walled ceramic plates or tubes. On a sub-microscopic scale, ceramics are not homogeneous, and to understand the relationship of additives and impurities to properties it is necessary to consider foreign ions that are in the crystal grains, in the grain boundaries, and in the surface. Surface studies on Na $\beta$ -alumina ceramics show the foreign species fall into three categories: 1) heavy metal impurities, 2) by-products of atmospheric corrosion, 3) excess or deficient 'non-stoichiometric' sodium.



The first category is typified by heavy metals, such as W and Fe, which may deposit during forming and firing and extend several  $\mu\text{m}$  below the surface. The second category is hydrogen, present in the surface as chemisorbed  $\text{H}_2\text{O}$  or  $\text{OH}^-$ . Hydrogen in the near-surface layers of Na $\beta$ -alumina ceramics can be bound by strong chemical bonds and we have found it to be retained at 400°C and  $10^{-6}$  torr. Measurements of Na concentration depth profiles using NRA are useful for studying the distribution in ceramics of non-stoichiometric sodium, a term used here to refer to Na concentrations greater than or less than single crystal compositions. The atom fraction of Na in the near-surface layers may differ substantially from that in single crystals of Na- $\beta$  and  $\beta'$  alumina. Examples of Na depth profiling on ceramic tubes that were known from x-ray diffraction to be mixtures of Na- $\beta$  and  $\beta'$  alumina are given in Fig 6. Below a  $\mu\text{m}$ , the Na concentrations are uniform and intermediate to those of crystals of the pure phases. However, in the near-surface layers, the Na concentration in one of the ceramics is equal to that in pure Na $\beta$ -alumina and the concentration in the other ceramic is extremely high, showing it is contaminated with a Na-rich phase, probably sodium meta-aluminate or sodium hydroxide.

#### $\beta\text{-PbF}_2$

$\beta\text{-PbF}_2$  is being studied by channeling at high temperature for insights into positional and thermal disorder of the conduction ions.  $\beta\text{-PbF}_2$  is among the best anion conductors known to date.

Although it has been the subject of several x-ray and neutron diffraction investigations, there is still confusion in the literature about the location of the F ions (7)(8). Channeling is interpreted by a physical model that does not involve phase relationships between the scattering centers, and it therefore offers an alternative technique for examining structure disorder in a lattice. The widths of the angular scans and the minimum yields are related to the positions and vibrations of the atoms in the atomic rows. To investigate the mechanism of the superionic conducting transition in  $\text{PbF}_2$ , simultaneous measurements of Pb and F channeling are being made as a function of temperature with a proton beam incident on the  $\langle 100 \rangle$ ,  $\langle 110 \rangle$ , and  $\langle 111 \rangle$  directions. An example of  $\langle 110 \rangle$  channeling by Pb and F at 590K is given in Fig 7. The channeling measurements support the fluorine disorder models that have been proposed to explain diffraction data.

### Discussion

There are numerous ways in which ion beam analysis can be used to study ionic conductors, including analyzing the composition of single crystals, determining composition depth profiles of dopants and impurities in the near-surface layers of ceramic electrolytes, and studying structure disorder and defects by channeling. The results obtained on Li and Mg doped crystals show it is possible to determine the composition of a single, small crystal. Solid electrolytes typically are non-stoichiometric and they exist over extended ranges

of chemical composition. The composition-stability relationships are not well known in many systems and it should be possible to clarify the phase diagrams by using particle scattering to determine the composition of very small crystals.

Our experience has shown that the composition in the near-surface layers of ceramic electrolytes can, and usually does, differ from the interior. Depth profile analysis to determine composition gradients as a function of distance from the surface is useful for studying the diffusion of impurities to and from the ceramic interior and reactions with the environment.

There should be no difficulty extending ion implantation to a wide variety of ions and solid electrolytes. Ion implantation inevitably introduces damage in the target but the results on Mn-implanted Na $\beta$ -alumina indicate radiation damage may not be a serious problem for the disorder can be removed by annealing at moderate temperature. To understand the effects of ion implants on the properties of superionic conductors, methods will have to be devised for determining the structure and properties in the near-surface layers. We are planning to use SEXAFS and channeling for this.

#### Acknowledgement

This work was supported in part by the Office of Naval Research.

## References

- (1) Ion Beam Handbook for Material Analysis , J.W. Mayer, E. Rimini, Eds., (1977) Academic Press
- (2) W.L. Roth, R.E. Benenson, V.K. Tikku, J.L. Briant, and B. Dunn, Solid State Ionics (1981) 5 , 163-166
- (3) J.T. Kummer in Progress in Solid State Chemistry , H. Reiss and J.O. McCalden, eds., Pergamon, N.Y., (1972) 1 , 141
- (4) W.L. Roth, F. Reidinger and S.J. LaPlaca in Superionic Conductors , G.D. Mahan and W.L. Roth, eds. (1977) Plenum, New York
- (5) J.D. Jorgensen, J.J. Rotella, and W.L. Roth, Inter. Conf. on Fast Ionic Transport in Solids, Gatlinburg (1981)
- (6) R.E. Benenson, W.L. Roth, V.K. Tikku, and P.J. Cong, Solid State Ionics, (1981) 5 .
- (7) K. Koto, H. Schulz, and R.A. Huggins, Solid State Ionics 3.4 (1981) 381-4
- (8) M.H. Dickens, W. Hayes C. Smith and M.T. Hutchings, in Fast Ion Transport in Solids , eds. P. Vashishta J.N. Mundy and G.K. Shenoy, North-Holland (1979)

# FIGURE CAPTIONS

Fig 1. RBS spectra of Na $\beta$ -alumina implanted with  $1.1 \times 10^{17}$

Mn<sup>+</sup>/cm<sup>2</sup> at 110 KeV. Solid line, as-implanted.

Dash-dot line, annealed 30 min. Dashed line, annealed 25 hr.

Fig 2. RBS spectra of Na $\beta$ -alumina: Solid line, random spectrum. Dashed line, aligned spectrum.

Fig 3. RBS spectra of Mn-implanted Na $\beta$ -alumina: Solid line, random spectrum. Dashed line, aligned spectrum.

Fig 4. Backscattering yields as a function of angle across  $\langle 0001 \rangle$  channel: X= Al yield, unimplanted crystal.  $\Delta$ =Al yield, implanted crystal. O=Mn yield, implanted crystal. The implanted crystal was annealed 30 min at 1100°C.

Fig 5. RBS spectra of Mn-implanted Na $\beta$ -alumina, annealed for 30 min at 1100°C.

Fig 6. Sodium depth profiles in near-surface layers of Na $\beta$ -alumina ceramics. The solid and dashed lines were measured on the inside and outside surfaces of the cylindrical, closed-end tubes.

Fig 7. Proton channeling in  $\beta$ -PbF<sub>2</sub> at 590K. Backscattering yields of Pb and F as a function of angle across  $\langle 110 \rangle$  channel.

BACKSCATTERED YIELD, ARITRARY UNIT

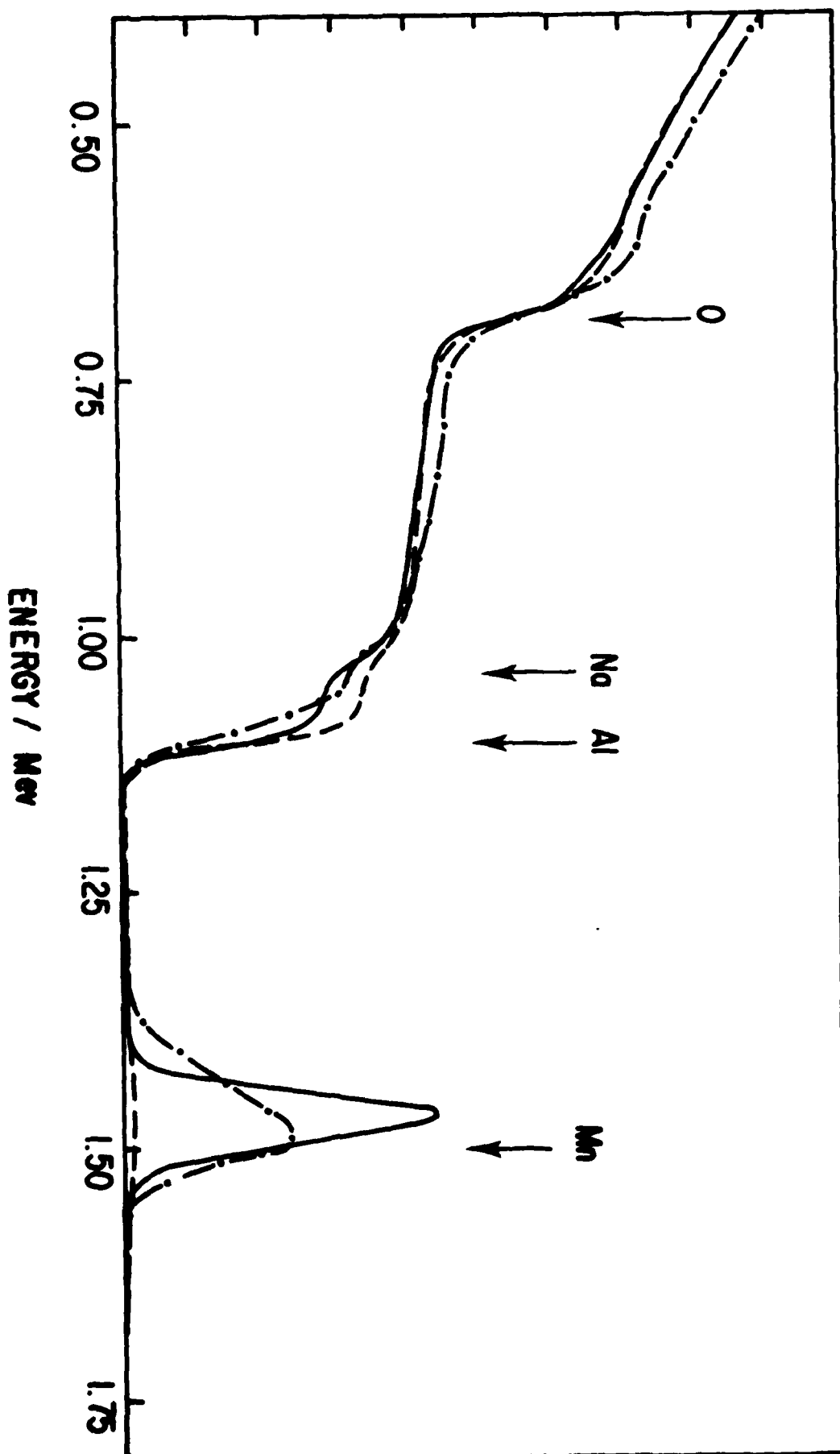


Figure 1

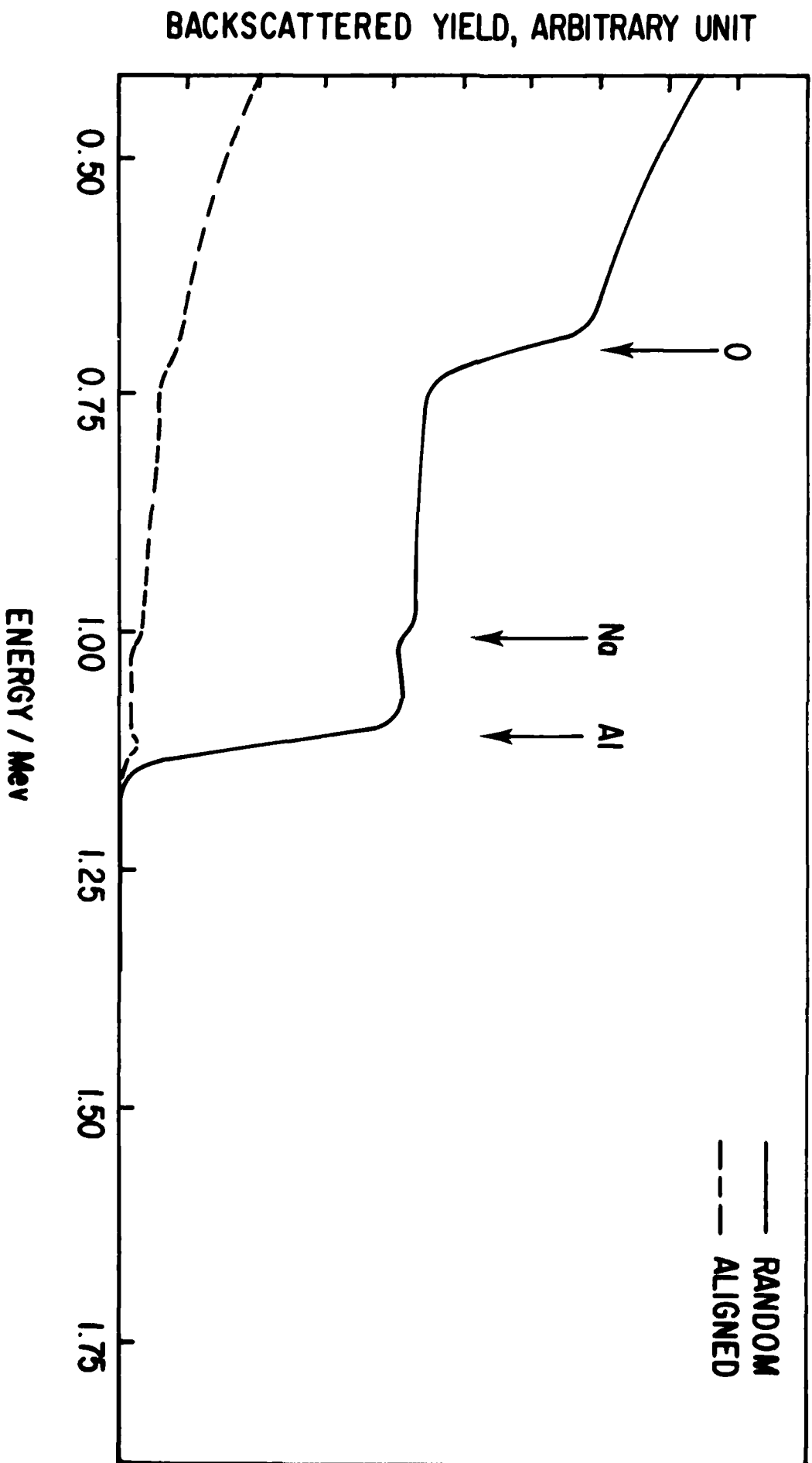


Figure 2

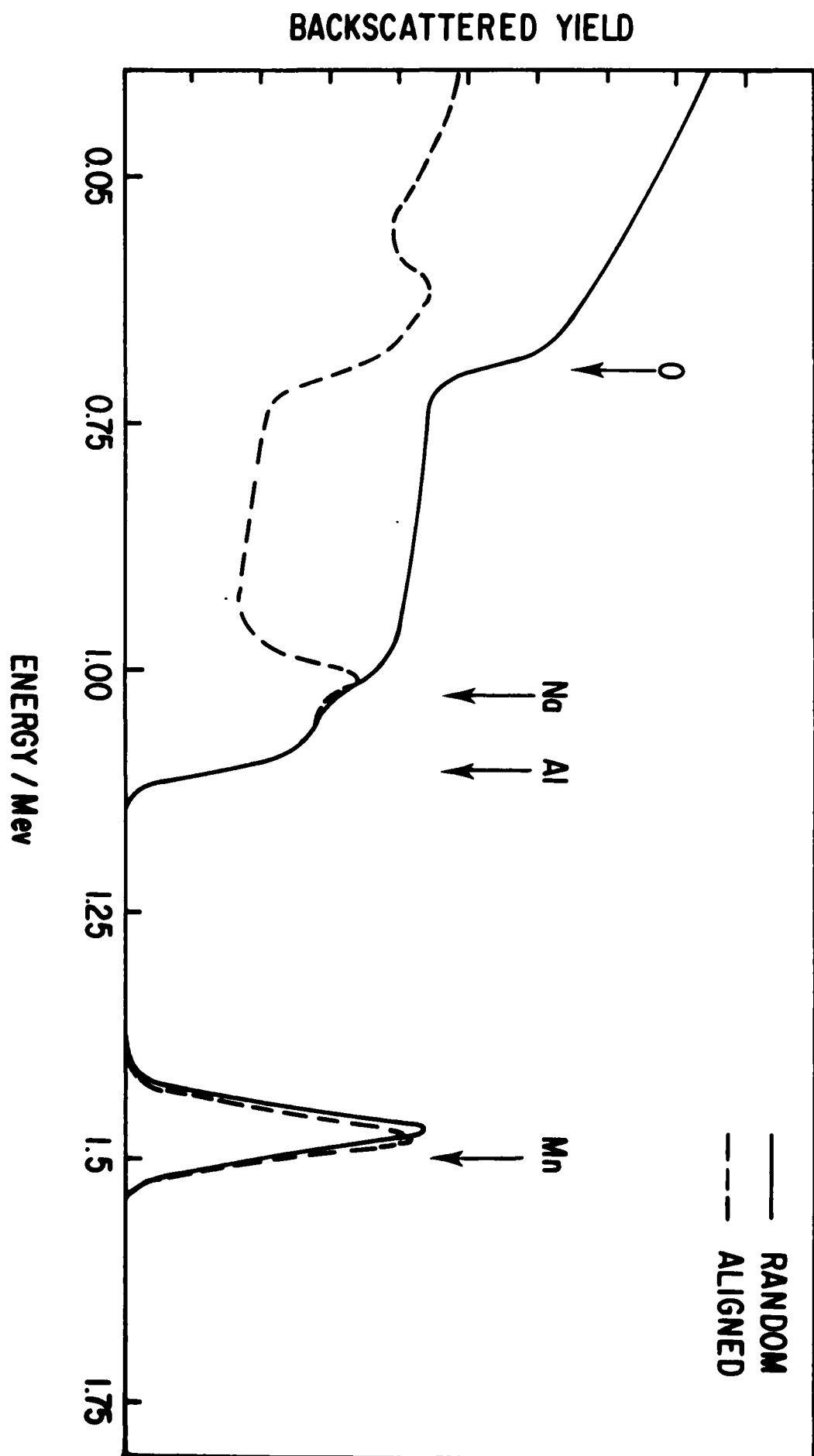


Figure 3



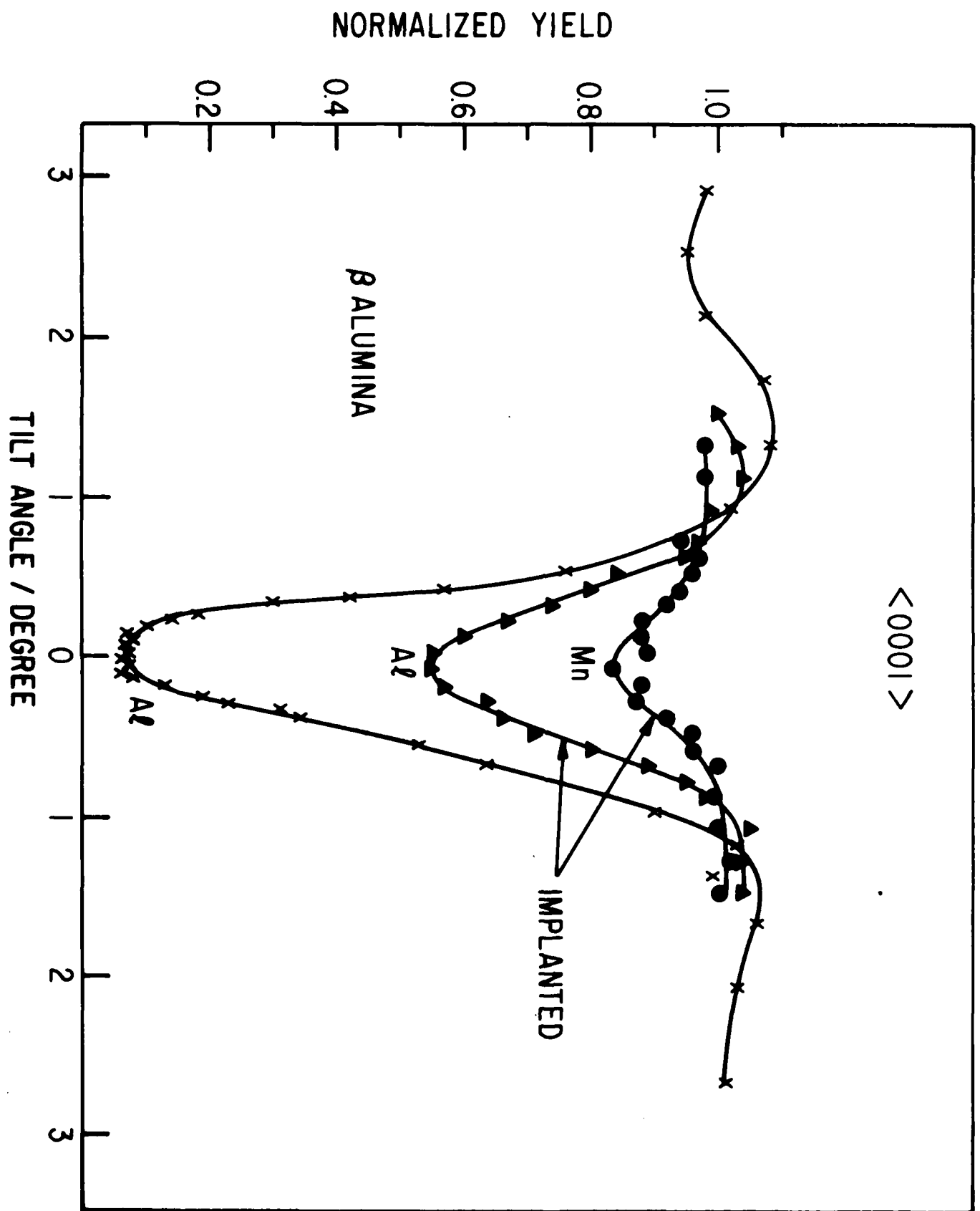


Figure 4

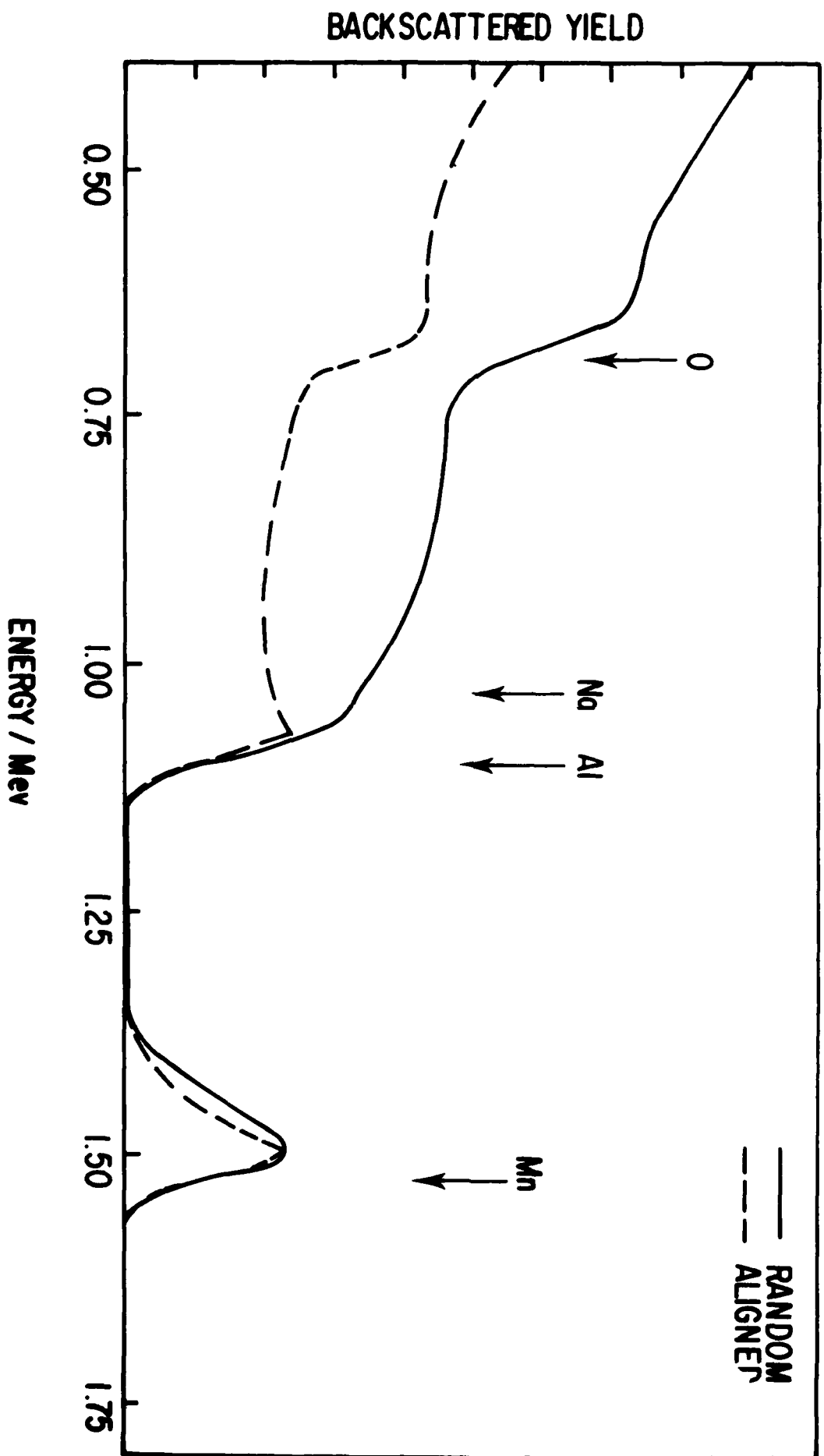


Figure 5

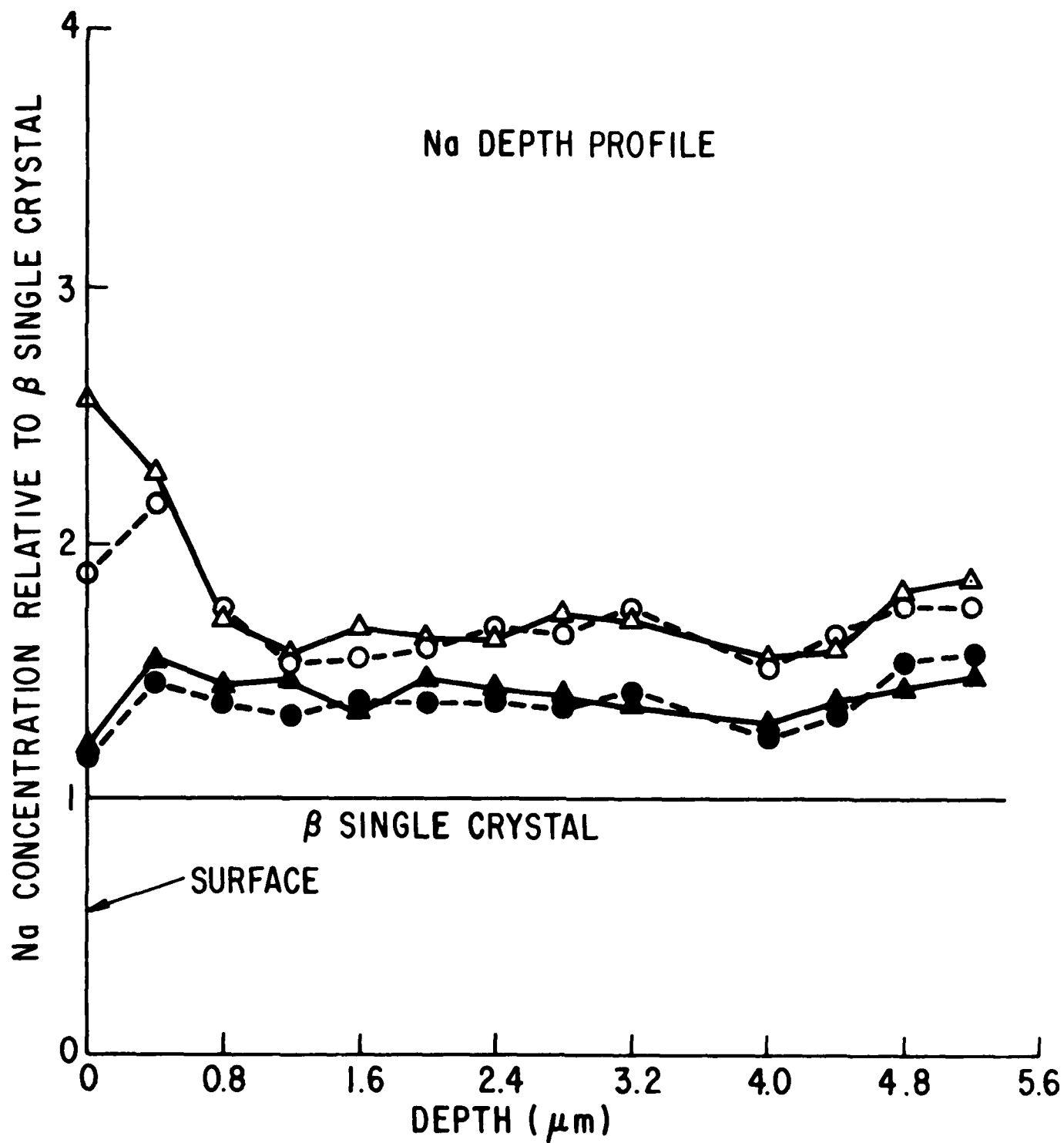


Figure 6

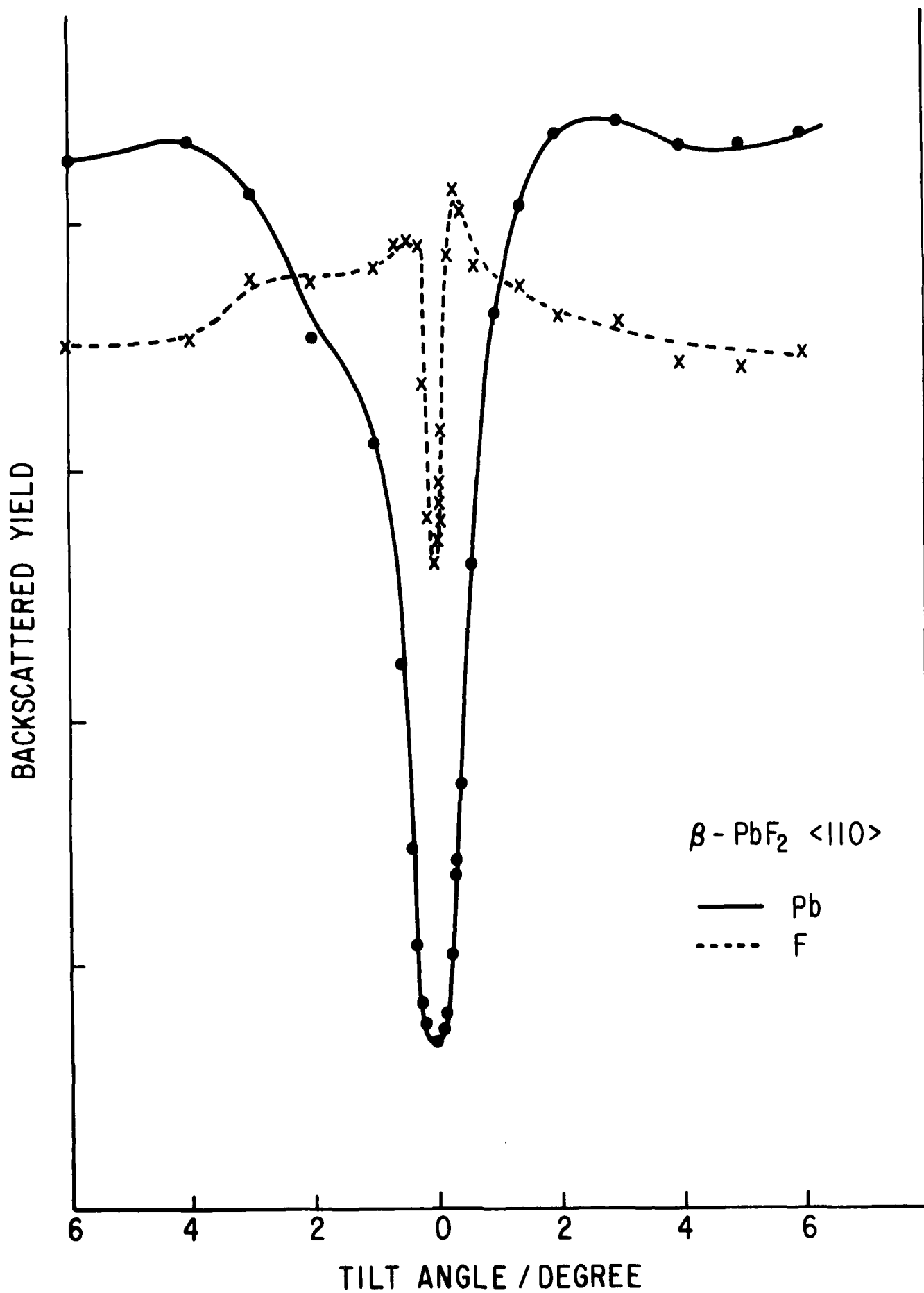


Figure 7

